

Numerical Estimation of Incident Wave Parameters Based on the Air Pressure Measurements in Pico OWC Plant

I. Le Crom¹, A. Brito-Melo¹, F. Neumann¹ and A. Sarmiento^{1,2}

¹Wave Energy Centre,
Av. Manuel da Maia, 36, r/c D., Lisbon 1049-001, Portugal
E-mail: izan@wave-energy-centre.org
E-mail: ana@wave-energy-centre.org
E-mail: frank@wave-energy-centre.org

²Instituto Superior Técnico,
Av. Rovisco Pais, 1, Lisbon 1000-201, Portugal
E-mail: antonio.sarmiento@ist.utl.pt

Abstract

The present study aims at assessing the key spectral parameters of the incident wave on a fixed oscillating water column (OWC) device, based on the air pressure measurements inside the chamber and on the numerical hydrodynamic coefficients of the device.

The methodology is based on the equation of continuity of the air in the time-domain and linear decomposition of the air flow in the usual terms of radiation and diffraction flows. By applying the Fast Fourier Transform, the time-domain equation is transposed to the respective frequency-domain equation.

This methodology was applied to the 400 kW OWC power plant, on the Island of Pico, Azores, which has been monitored since 2005 by the Wave Energy Centre. The numerical hydrodynamic coefficients obtained by the 3D radiation-diffraction boundary element code, AQUADYN-OWC, were used in this study.

No measurements of the incident wave in front of the plant are available; therefore the results obtained for a set of records are compared with forecast estimations for the site of Pico plant provided by INETI and also with the measurements of two directional wave rider buoys offshore Pico and Terceira islands. These data are provided by the Centre of Climate, Meteorology and Global Changes and propagated via the SWAN spectral wave model to the zone of interest.

Final objective is to improve the control of the Pico plant by assessing its performance for a range of sea states.

Keywords: Numerical Modelling, Pico OWC Plant, Wave Climate, radiation, diffraction, frequency domain

Nomenclature

V_0	= average volume of the chamber
γ	= ratio of specific heats, c_p/c_v
$q_i(t)$	= volumetric flow rate
$q_d(t)$	= diffraction flow
$q_r(t)$	= radiation flow
ω	= frequency (rad/s)
$P(\omega)$	= complex amplitude of the air pressure
$Q_D(\omega)$	= complex amplitude of the diffraction flow
$Q_R(\omega)$	= complex amplitude of the radiation flow
$A(\omega)$	= complex amplitude of the incident wave
$H_D(\omega)$	= transfer function of the diffraction problem
$H_R(\omega)$	= transfer function of the radiation problem
$S(\omega)$	= frequency spectral density
m_n	= n^{th} spectral moment
H_s	= significant wave height
T_z	= mean zero-crossing period
T_e	= energy period

1 Introduction

Pico plant Monitoring

An oscillating water column OWC wave energy device consists of an air chamber in which the front wall has an opening so as to let waves enter inside. The wave action makes the water level in the air chamber to oscillate and the air in the chamber is compressed and expanded generating an air flow through a turbine. The 400 kW European Wave Power plant at the island of Pico, on the Azores, is of this type. It is a bottom-mounted device equipped with a fixed-blades Wells turbine with a guide vane stator on each side of the rotor. To avoid over-pressure and stall conditions, a relief valve exists which can be opened from 0% to 100%, according to the incident sea-state. The safety of the turbo-generation group is provided by redundancy in the closure mechanism of the air duct: a slow-acting guillotine-type isolation valve is shut whenever the

plant is non-operational over a longer period, whereas the fast-acting variable-pitch-blade manoeuvre valve can be efficiently operated during test periods.

The OWC plant is situated in a rocky shore on the Northern coast of Pico Island (Fig. 1). The bottom of the sea under the incident wave is around 8 m depth. The plant is exposed to waves from the directions including the best wave climates ($+30^\circ$ North to -60° North). The other directions are shadowed by two islands, São Jorge, Faial and Pico itself.

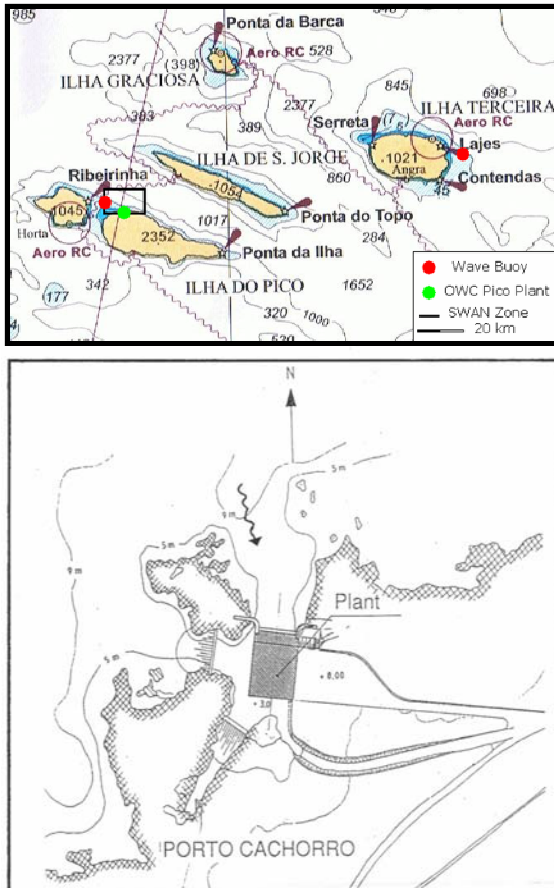


Figure 1: Location of the OWC Pico plant in Azores (on the top) and detail of the coastal area where the plant is installed (below)

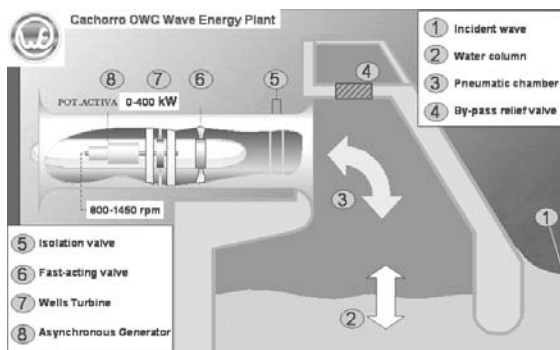


Figure 2: Essential components of Pico plant.

The air pressure inside the chamber is measured using one pressure transducer installed on the floor of the turbine room at level 8.20 m. The water level inside the chamber is measured with an ultrasonic transducer installed on top of the wave chamber, with access from the gallery. An absolute magnetostrictive linear position sensor was installed in the hydraulic piston to indicate the position of the relief valve.

In 2007 focus of the works on the Pico OWC was the identification of weak points in terms of plant operation and data acquisition (DAQ). The major issue has been the persisting vibration problem that however is outside the scope of this article. With respect to the data acquisition and control issues, the following features are being gradually implemented:

- (i) Identification of key parameters (physical quantities, sensor setup, software, integration of PLC and scientific data) for new DAQ system;
- (ii) Design of additional safety shut-down mechanism independent of the plant PLC (deemed required for autonomous operation);
- (iii) Design of automatic relief valve adjustment based on local incident wave measurements.

The most relevant of these for the work presented in this article is the last item, as it delivers reliable real-time wave elevations in the direct vicinity of the plant. However, due to funding gaps, this and the other items had to be dealt with in-house with minimum means, and are not fully implemented to date. Consequently, to date no direct measured data is available for the wave resource in front of the plant.

Sporadic information on the wave climate has been collected with an offshore directional wave rider buoy, located between Faial (the closest island from Pico) and Pico islands (hereafter ‘Channel Buoy’), through the CLIMAAT Project (Climate and Meteorology of the Atlantic Archipelagos) [1]. Further, reasonable resemblance of data can be expected from the wave rider buoy located close to Terceira Island (hereafter ‘Terceira Buoy’; also CLIMAAT project), which is 80 nautical miles east of the Cachorro site and has shown better availability than the Channel Buoy. Forecast data offshore and in front of the plant is provided by INETI/LNEG, as well as offshore predictions carried out by the Windguru website. All this available information was used to validate the methodology here presented to estimate the incident wave parameters.

Pico plant Numerical Modelling

In the scope of the Pico plant project two different tools have been developed:

- i) a wave-to-wire model of fixed OWC devices based on the linearised version of the continuity equation applied to the air inside the pneumatic chamber which can be used to assess the performance of the plant for a set of different sea states [2];
- ii) a modified version of the 3D radiation-diffraction boundary element code, AQUADYN (École Centrale de Nantes), originally for the hydrodynamic study of floating bodies [3]. The

adaptation to the OWC consisted in the incorporation of a boundary condition in the internal free surface of the pneumatic OWC chamber to take into account of the pressure fluctuation [4]. This modified version can be used for the frequency domain analysis of the OWC, namely to compute the hydrodynamic coefficients and excitation flow.

Based on the dimensions of the Pico wave power plant and on data of the bathymetry area around the plant the meshed body has been obtained [5] as presented in Fig 3. In the remaining part of the domain (not discretised) a uniform depth of 7.8 meters (mean water level in situ) was assumed. AQUADYN-OWC was used to compute the transfer functions of the radiation and diffraction problems. A comparison study between the numerical curves and the experimental evaluations (1:35 scale model tests) has been performed [5] which allowed to verify that there is reasonable agreement between those results. Although some aspects that may influence this comparison were pointed out:

- Viscous effects and other non-linear hydrodynamic effects are not taken into account in the numerical modelling.
- The physical model the coastline is not hundred percent reflective, contrary to the numerical simulation case, where the coastline is assumed to be fully reflective.
- There are some geometrical differences between the scale model and the meshed body for the numerical computations.
- The depth for the numerical model was assumed to be 7.8 m, which is the mean depth in the vicinity of the plant, whereas in the scale model the bathymetry was drawn out until a depth of 12 m.

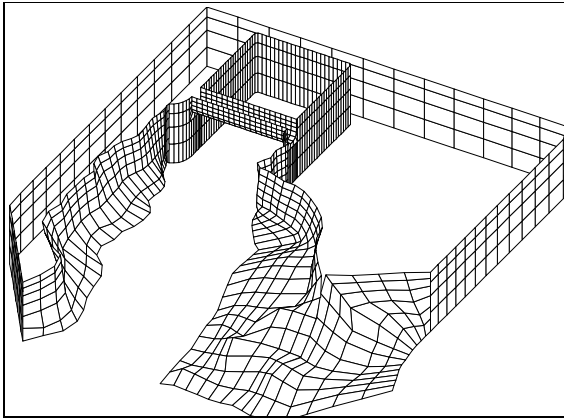


Figure 3: Discretization of the Pico plant

The aim of this paper is to develop and validate a mathematical tool for estimating the wave incident parameters using the numerical transfer functions of the radiation and diffraction problems and the air pressure measurements inside the chamber. This methodology is presented in the following section.

2 Mathematical model

Hydrodynamic modelling in the time domain

The hydrodynamic model is based on the pressure model presented in [5]. The linearised version of the continuity equation applied to the air inside the pneumatic chamber is given by

$$q_t(t) + q_v(t) = q(t) - \frac{V_0}{\gamma P_a} \frac{dp(t)}{dt}, \quad (1)$$

where $q_t(t)$, $q_v(t)$ and $q(t)$ are respectively, the volume flow rate through the turbine, the volume flow rate through the relief valve and the volume flow rate displaced by the free-surface inside the chamber. V_0 denotes the volume of the air in the chamber under undisturbed conditions, P_a is the atmospheric pressure and γ the ratio of specific heats (equal to 1.4). According to the linear water wave theory, the volume flow rate displaced by the free-surface inside the chamber may be decomposed as

$$q(t) = q_d(t) + q_r(t), \quad (2)$$

where $q_d(t)$ is the diffraction flow rate, due to incident wave action assuming the chamber at constant atmospheric pressure, and $q_r(t)$ is the radiation flow rate due only to the pressure oscillation $p(t)$ in otherwise calm waters. When the turbine is not operating and the relief valve is closed it turns that:

$$q_d(t) = \frac{V_0}{\gamma P_a} \frac{dp(t)}{dt} - q_r(t). \quad (3)$$

Hydrodynamic modelling in the frequency domain

According to linear theory, the interactions between waves and the OWC device may be represented by transfer functions in the frequency domain. The diffraction flow may be related to the incident wave elevation, A , at the point (x_0, y_0) , by means of a diffraction transfer function:

$$H_D(\omega, x_0, y_0) = \frac{Q_D(\omega)}{A(\omega, x_0, y_0)}. \quad (4)$$

The radiation flow can be related with the derivative of the air pressure inside the chamber by the radiation transfer function:

$$H_R(\omega) = -\frac{Q_R(\omega)}{i\omega p(\omega)}. \quad (5)$$

The complex amplitudes in frequency domain are related with the time domain quantities by means of:

$$p(t) = P(\omega)e^{-i\alpha t}; \quad (6)$$

$$q_d(t) = Q_D(\omega)e^{-i\alpha t} = AH_D e^{-i\alpha t}; \quad (7)$$

$$q_r(t) = Q_R(\omega)e^{-i\alpha t} = (-i\omega P)H_R e^{-i\alpha t}. \quad (8)$$

Replacing (7) and (8) in (3), the complex amplitude of the incident wave can be expressed as:

$$A = \frac{i\omega P H_R - i\omega P \frac{V_0}{\gamma P a}}{H_D}. \quad (9)$$

This expression allows to compute the complex amplitude of the incident wave using the numerical estimates of transfer functions of radiation and diffraction problems and the complex amplitude of the air pressure (obtained by Fourier Transform of the corresponding time series measured inside the chamber). This expression can only be used when all valves are closed and the turbine is not operating.

The frequency spectral density, $S(\omega)$, is determined by

$$S(\omega)\Delta\omega = \frac{1}{2} A^2. \quad (10)$$

A selection of spectral parameters is typically used to characterize a sea state. The significant wave height, mean zero-crossing period and energy period are defined respectively by

$$H_S \cong 4\sqrt{m_0}, T_z = \sqrt{m_0/m_2}, T_e = \frac{m_{-1}}{m_0}.$$

With the n^{th} moment of the frequency spectrum defined as ($\omega = 2\pi f$):

$$m_i = \int_0^{\infty} f^i S(f) df.$$

3 Methodology

This section presents the methodology used in this study, taking as an example a record of half an hour of the pressure measurements inside the chamber (the acquisition data is 0.2 s), when the chamber is fully closed (Figure 4).

By applying the Fast Fourier Transform to the measured pressure time series, the respective Pressure Spectrum is obtained as presented in Fig. 5, with a sampling frequency equal to 5 Hz. We are able to reconstitute the spectrum until the Nyquist frequency (2.5 Hz or 15.7 rad/s), i.e., over a wider domain than the one as presented in the figure below. However the range of frequencies was limited by two reasons: First, the numerical estimates of H_D and H_R (see Fig. 6) were computed for the range of frequencies between 0.18 and 2.5 rad/s (respectively 0.028 and 0.4 Hz). Secondly when using (9), values of H_D close to zero (for frequencies above 1.6 rad/s) are responsible for meaningless peaks.

Therefore the study was limit to a range of angular frequencies between 0.18 and 1.58 rad/s (0.028 to 0.25 Hz) to avoid the division by zero. This limitation still allows the study of swell periods between 4 to 35 s.

Further the numerical transfer functions computed with a frequency width of 0.02 rad/s were interpolated in order to fit with the FFT of the pressure measurements (frequency width of 0.0035 rad/s).

The wave spectral density obtained from (9) and (10) is presented in Fig. 7.

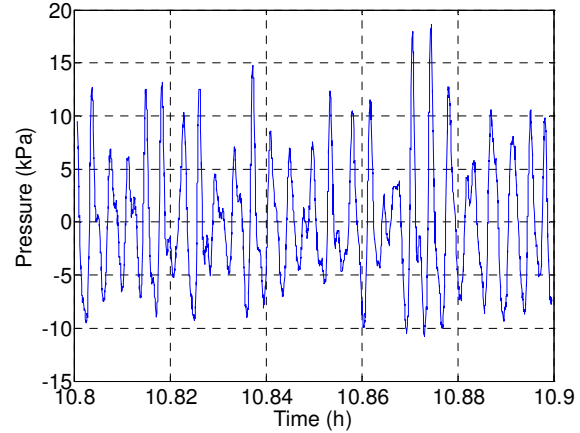


Figure 4: Time series of the air pressure recorded inside the chamber (2009.04.05); Conditions: turbine not running and air valves closed

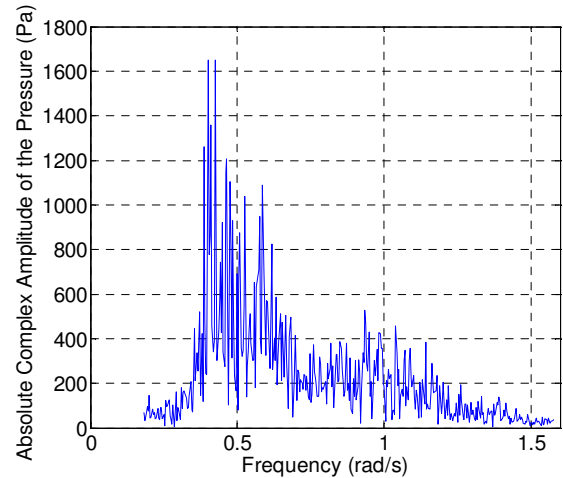


Figure 5: Spectrum of the air pressure inside the chamber

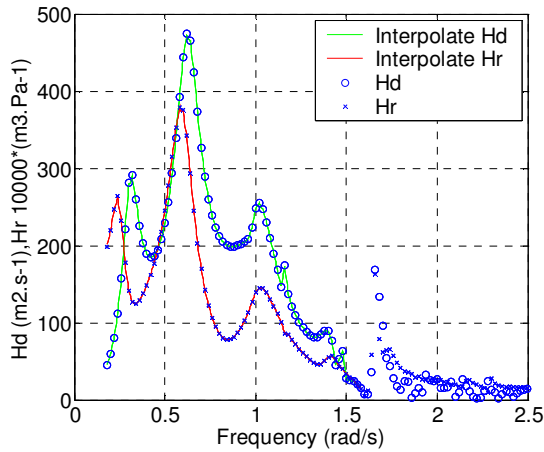


Figure 6: Diffraction and radiation transfer functions modulus

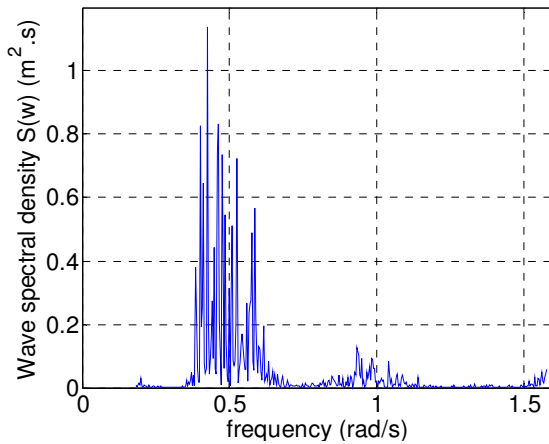


Figure 7: Estimated wave spectral density

By calculating the zero order and negative order of the spectral moments, the significant wave height, mean zero-crossing and energy period are obtained, respectively:

$$H_s = 1.03 \text{ m}, T_z = 10.10 \text{ s}, T_e = 12.11 \text{ s}.$$

These results can be compared with the wave rider buoy close to Terceira, one hour later (Table 1):

Date	Time [h]	Hs [m]	Hmax [m]	Tz [s]	Tmax [s]	Dir* [°]
05/04/2009	11.5	1.24	1.83	7.5	15.6	361

Table 1: “Terceira” Wave Buoy data.

N.B*: All wave directions are defined according to the nautical convention, i.e., the direction where the waves come from, measured clockwise from geographic North.

When comparing the estimated wave parameters with the information provided by the wave rider buoy it is important to point out that: In (9) the amplitude of incident wave far away from the coast is not disturbed by the coast. The depth for the numerical model was

assumed to be 7.8 m, which is the mean depth in the vicinity of the plant. It is assumed that the incident wave characteristics we are assessing correspond to the wave climate at 7.8 m water depth.

Furthermore the calculated period may be affected by the cut of frequency.

Applying the IFFT to the complex amplitude of the incident wave we obtain its surface elevation which can be compared with the surface elevation measured in the chamber as presented in Fig. 8. The measurements of the water free surface elevation inside the chamber are generally higher than the incident wave elevation due to the resonance phenomenon that occurs in the chamber.

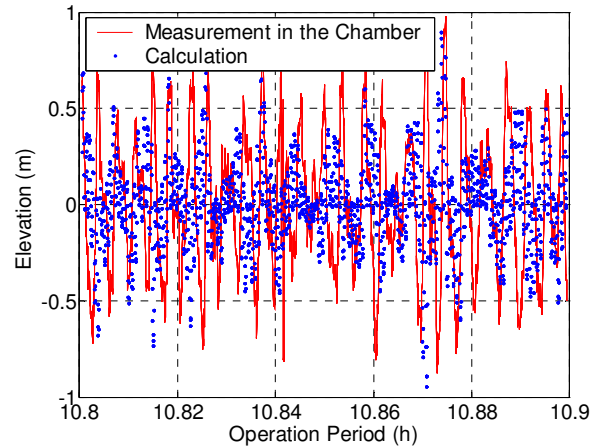


Figure 8: Calculated water free surface elevation of the incident wave (dots) and water free surface elevation measured inside the chamber (line)

4 Validation of the method

The tests used to validate this study are those in which the pressure is measured with the generator switched off and the relief valve closed so that the (9) can be applied. These conditions were not frequent in the period from 2005 to 2008 because in general when the plant is not operating, the relief valve is open for security reasons. Therefore just a few time series could be used. In 2007 an accident occurred: one part of the turbine duct broke during the operational period and while the fibre duct was replaced, several useful measurements have been performed. Those measurements allowed a first comparison to be carried out.

October 2007 – November 2007

Fig. 9 and Fig 10 present the comparison between the available data (offshore directional wave rider measurements, offshore predictions and forecasts in front of the plant) with our numerical estimates of significant wave height and period. Fifteen tests were used with durations between 20 to 50 minutes; the sampling frequency was 2 Hz.

The offshore directional wave rider buoy, located between Faial and Pico islands - Channel Buoy - was not all the time available and only in four days (12th, 22th, 29th and 30th October 2007), the pressure with the chamber fully closed was acquired.

During the period October 2007 and beginning of November, the mean wave direction was in the range 314° - 22°, with no “obstacles” to the incoming waves. Therefore the data from the wave rider buoy is comparable with the results obtained.

The buoy is located 9 km offshore the plant. SWAN model will be applied to the wave field until the 8 m water depth in front of the plant. The wave rider data presented in Figs. 9 and 10 concerns offshore data without taking into account propagation effects to the plant. The forecast data provided by the INETI assesses the wave characteristics in front of the plant. The offshore Windguru forecast is only used quantitatively since the location of the Windguru data is unknown.

We observe that the numerical estimates of H_s are in general lower than the available data from the Channel buoy and Windguru forecasts, as expected because these concerns offshore data. However the results follows the same tendency as the Channel buoy. According to the information provided by the coordinator of CLIMAAT project [1], the buoy was shut down for lower waves for the purpose of saving its memory. The comparison improves when comparing with the forecast data (from INETI) in front of the plant. For the periods it is more difficult to visualise a similar tendency due to the lack of available data. Because of the limitation in frequency mentioned in previous section the estimated mean zero-crossing period is surely biased and we will prefer the energy period, less sensitive to the high frequency (comparable with the buoy data and INETI forecast). Nonetheless the order of magnitude is matching quite well between the buoy records and our estimations.

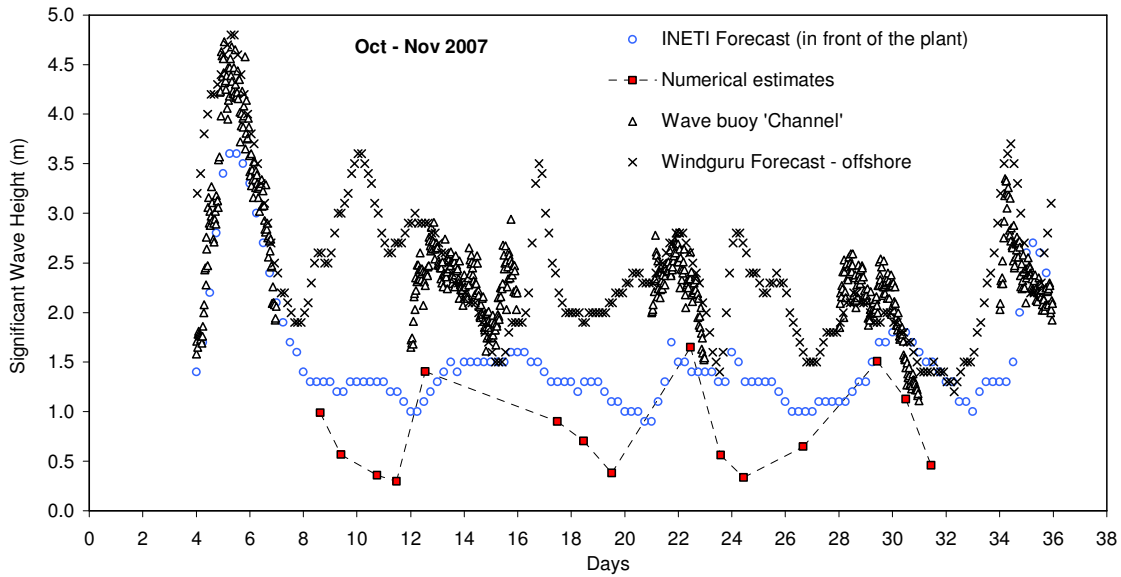


Figure 9: October 2007 - beginning of November 2007 – H_s

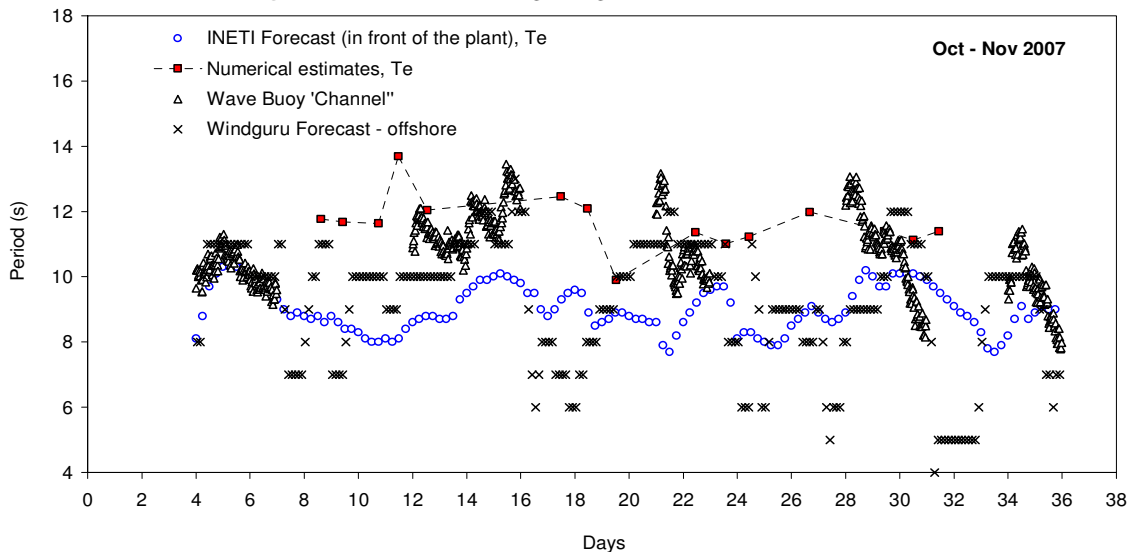


Figure 10: October 2007 - beginning of November 2007 – Period

April 2009

A similar comparison is performed in Fig. 11 and 12. More than 100 tests were used with durations of 30 minutes; the sampling frequency was 5 Hz.

The offshore wave rider buoy, located between Faial and Pico islands, “Channel Buoy”, was not available. Consequently the offshore wave rider “Terceira buoy” was used. Online data is only available every 5 hours.

During the month of April 2009, the mean wave direction was always in the range between 350° and 10°, with no “obstacles” to the incoming waves. Therefore the data from the wave rider buoy is comparable with the results obtained. The buoy is located 130 km far from the plant. Fig 11 and 12 present the offshore results without taking into account the propagation until the plant (the bathymetry was not

available for the local where this buoy is located). Again it is observed that the numerical estimates of H_s are lower than the available data from “Terceira buoy”, as expected because this is an offshore measurement. This is more remarkable for high waves between 1.8 to 2.8 m or low waves below 1.2m. When comparing with the forecast data in front of the plant (from INETI) and the forecast data offshore (from Windguru) the agreement is not very good.

In what concerns the comparison of periods, in general one can observe a same tendency of the numerical estimates and “Terceira buoy”, as well as with the forecasts data. Notice that the period recorded by the wave rider buoys is the mean zero-crossing period; the period from INETI forecasts concerns the energy period; from the Windguru data it is unknown what period is recorded;

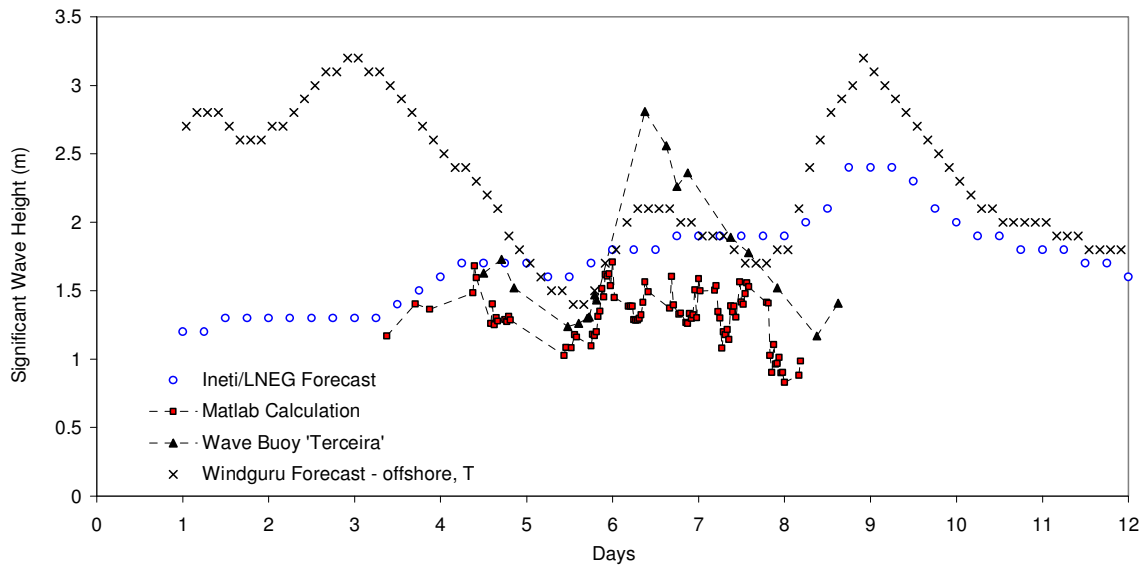


Figure 11: April 2009 – H_s

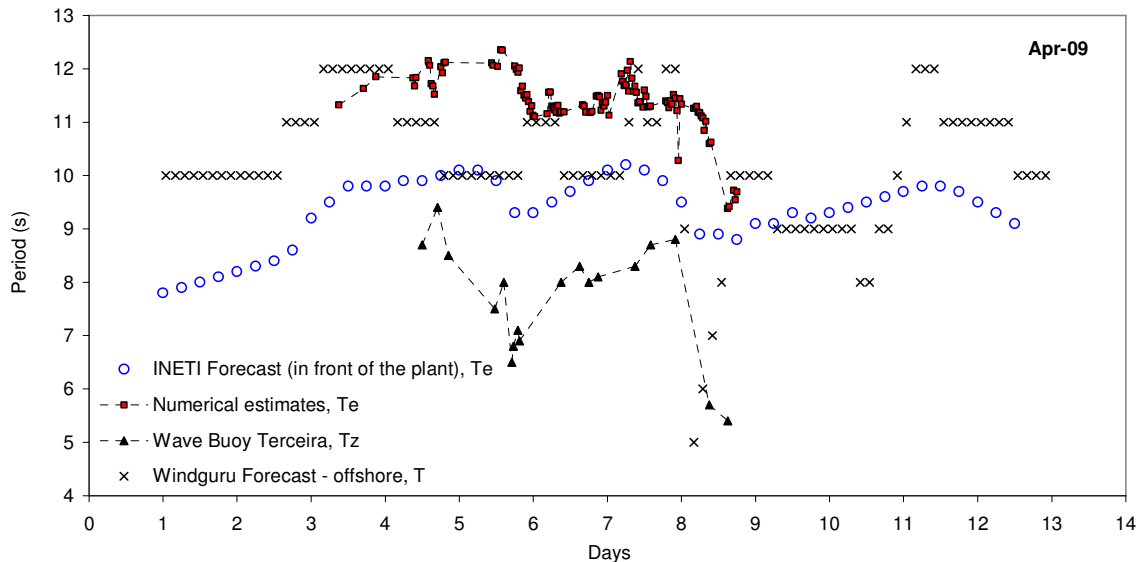


Figure 12: April 2009 - Period

May 2009

A similar study was done for the first days of May. Results are compared in Fig. 13 and Fig. 14. The “Channel Buoy” was not available and therefore “Terceira Buoy” was used. Online access was every hour. During the month of May 2009, the mean wave direction varied between 318° to 73° . When the incoming waves are characterized by a northeast mean direction the plant is shadowed by São Jorge Island and

the buoy records and the measurements in the plant are no more comparable. In Fig 13 and 14 it is highlighted the days in which the incident waves are shadowed. We observe that the numerical estimates of H_s follows the same tendency as the “Terceira buoy” data, but are lower than the offshore measurements, as expected. Regarding the comparison between periods, in general one can observe that the numerical evaluations of energy period follow the same tendency as the “Terceira buoy” as well as the forecast data.

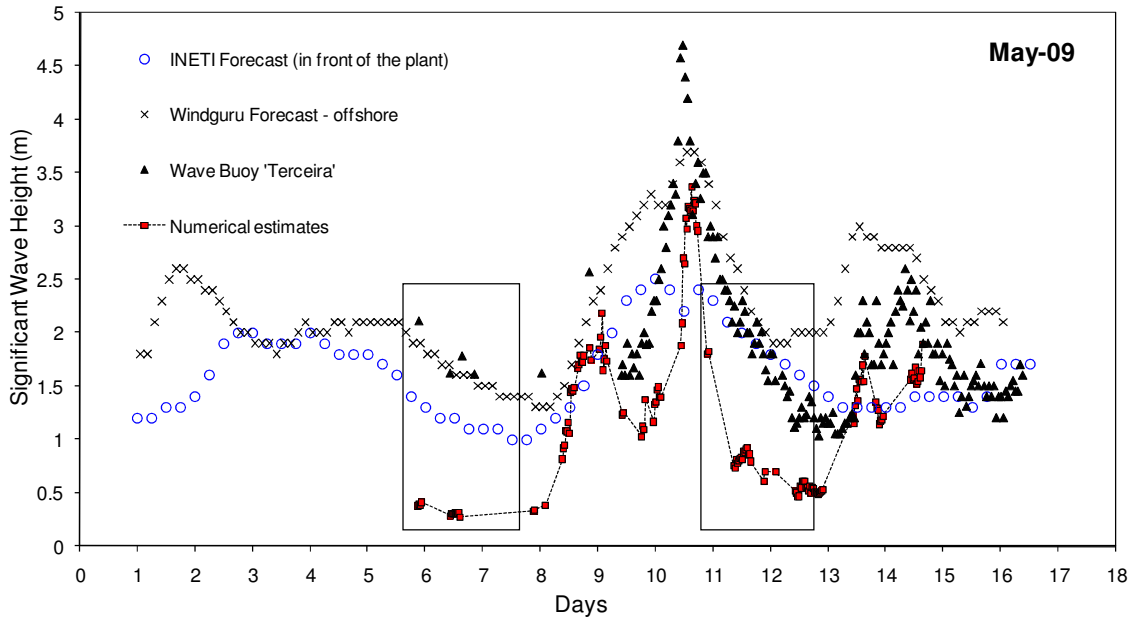


Figure 13: May 2009 – H_s (in the two rectangular areas the wave direction measured by the wave rider buoy is such that Pico plant is shadowed by São Jorge island)

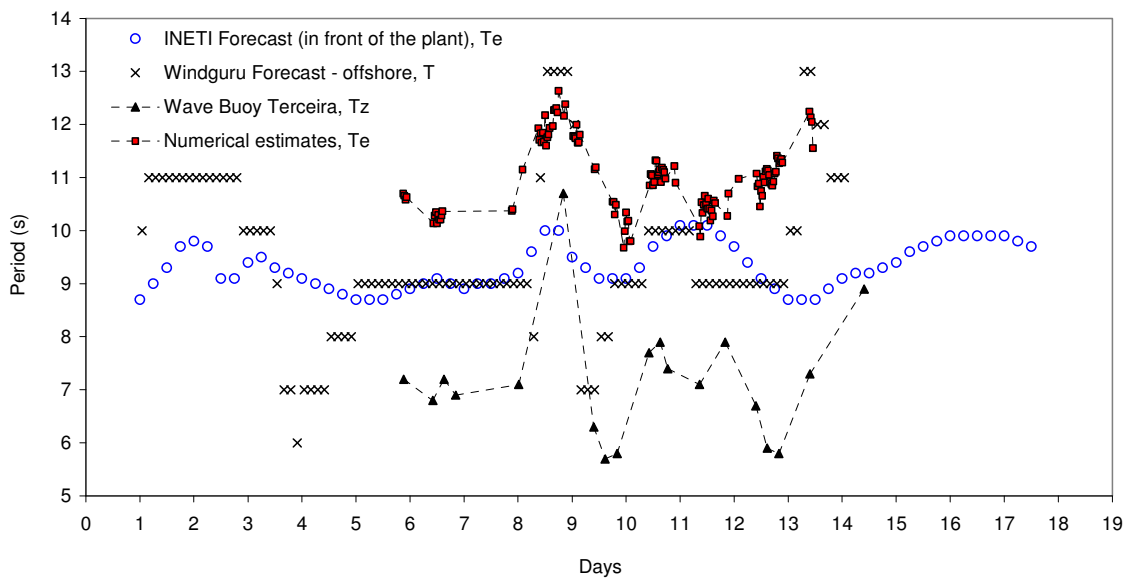


Figure 14: May 2009 - Period

5 Discussion

The results presented in the previous section were compared with data measured by wave rider buoys located offshore the island. However to improve this comparison the waves have to be propagated until the 7.8 m water depth (in front of the plant). This was done using SWAN code.

The bathymetry of this region was based upon 4 hydrographical charters of the Portuguese Instituto Hidrográfico, (1983 to 1995). The precision of the bathymetry is 15'' (roughly 460 m lat and 360 m long) and it represents an area of 16 x 12 km, called Swan zone (Fig. 1). Also information about the depth in front of the plant was used (WavEC in 1987). A first linear interpolation was carried out to obtain in a realistic way a more detailed bathymetry (Fig. 16). SWAN requires a bathymetric input grid with sufficient spatial resolution to ensure that all relevant features of the seabed are properly resolved. The software Alterabtim (developed by Hidromod, Lisbon, Portugal), was used to carry out an interpolation to achieve a resolution of 25 m for the all domain.

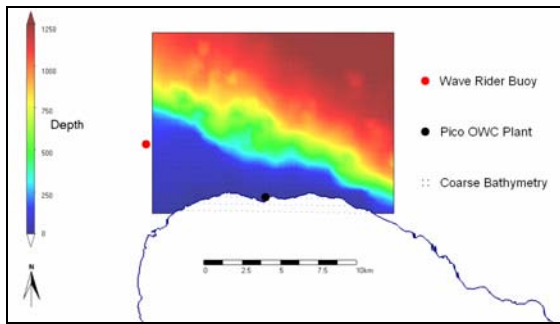


Figure 16: Reconstruction of the bathymetry

The offshore wave regime is based upon the observed wave data, i.e., the significant wave heights (H_s), mean wave directions (Dir), mean wave periods (T_z) and directional spreading ($Dspr$), between Pico and Faial Islands collected by the CLIMAAT Project [1]. The corresponding peak period (T_p) was calculated using the Jonswap spectrum (peak enhancement parameter = 3.3), which is the parameter used as input by the SWAN model. Wind, current, and tidal input grids were not generated. The current was therefore assumed to be zero and the tidal constant all over the grids. As the non-linear quadruplet interactions are not recommended to be used with zero wind conditions a weak and constant speed of 0.1m/s was assumed over both grids.

The boundary conditions were defined by using data output based on the directional wave rider Buoy. For every distinct sea states the wave climate is constant (uniform and stationary) along three sides of the input grid to fully enclose the zone of interest. The grid model was defined with 36 directional bins of 10°, covering all possible wave directions, and 32 frequency

bins. When input into SWAN, the boundary conditions were defined as JONSWAP spectra.

The model was set to output two sets of results:

- Significant wave height, mean period, wave direction and energy transport at 25m intervals across the whole domain (Fig. 17).
- Significant wave height, mean period, wave direction and wave spectrum at the front of the plant (8m water depth).

An example of results obtained for a reference state of $H_s = 1.5m$, $T_e = 8s$, $Dir = 295^\circ$, $Dspr = 25^\circ$ is shown in Fig. 17. This reference sea state has been chosen to show the effect of the refraction due to bathymetric change as the waves propagate shoreward because of a mean direction set to 295° . As expected, the propagation of the waves until the 7.8m water depth line shows a diminution of H_s (Fig. 17).

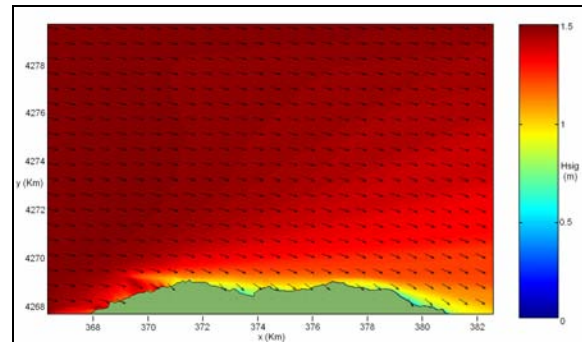


Figure 17: SWAN simulation: $H_s = 1.5m$, $T_e = 8s$, $Dir = 295^\circ$, $Dspr = 25^\circ$

As a realistic case of study results from the 29th May 2008 are presented in Table 2, between 3 PM to 4 PM. In this record we have one hour of pressure measurements with closed relief valve and turbine not operational which match with three half an hour length spectrum of the wave rider buoy analysed by the software w@ves21 (Datawell).

Location	Time [h]	H_s [m]	T_z [s]	T_e [s]	Dir [°]	$Dspr$ [°]
Channel	15h04	1.43	5.21	7.91	359	24.6
Channel	15h34	1.28	5.24	7.91	354	23.4
Channel	16h04	1.56	5.11	7.64	4	4.2

Table 2: Wave Buoy data before applying SWAN code.

Finally, to compare the two different spectra (calculated and measured) we imposed the same limitation of the frequency domain modelling (cut of frequency inferior to 0.18 rad/s and superior to 1.58 rad/s) to the spectrum obtained by using SWAN (Fig. 18). Table 3 presents the results after applying SWAN to the Channel Buoy compared with the numerical estimates.

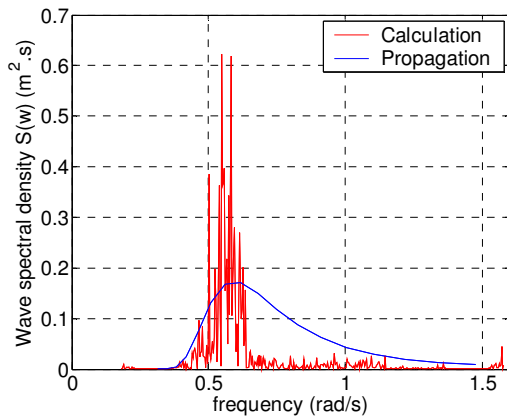


Figure 18: Comparison of the spectra.

Origin	Time [h]	Hs [m]	Tz [s]	Te [s]
Channel	15h04	1.14	6.67	7.17
Channel	15h34	1.07	6.65	7.14
Channel	16h04	1.21	6.55	6.98
Calcul	15h15	0.64	9.95	10.84
Calcul	15h45	0.71	9.74	10.78

Table 3: Wave Buoy data after the application of SWAN code and comparison with numerical estimates

Taking into account the wave propagation effects and the limitation of the frequency domain in the wave spectrum we found that it is not sufficient to explain the lower values of our numerical estimations. The reason for this may be caused mainly by the non-isolation of the chamber. In fact several leaks are known in the plant's walls. Finally this calculation seems to be correct but would not be fully verifiable before the reparation of the leaks, or before the assessment of the flow loss through them, because those holes are not structural and consequently not primordial for plant survivability.

6 Conclusions

In this paper a methodology was developed to estimate the incident wave parameters in front of a shoreline OWC power plant. The model was applied to the OWC Pico plant monitored by WavEC since 2005.

The mathematical model is applied under the conditions of chamber fully closed. The following are inputs for the mathematical model:

- Fourier transform of the time series of the air pressure recorded inside the chamber;
- Numerical estimates of the diffraction and radiation transfer functions computed in the frequency domain using a BEM code, such AQUADYN-OWC.

The model was validated comparing the numerical estimates with data available from two wave buoys located offshore, as well as with forecast data provided

by INETI, in front of the plant. Three set of records were analysed (October 2007, April 2009, May2009).

It can be concluded that there was a good agreement between the numerical estimation of Hs and the available data in terms of following a similar tendency although the precision of the obtained results remained below the expectations; several causes for this can be pointed out:

- Presence of leaks in the plant;
- Cut of frequency in the numerical calculations;
- Assumptions for the hydrodynamic coefficients computation (see introduction).

It should be noted that this is the first step of a comprehensive study. In order to improve the precision of the methodology presented in this paper, the following actions are suggested:

- Refinement of the local bathymetry
- Extension of the propagation study until Terceira
- Adaptation of the theory to an open relief valve situation or with an operating plant

Acknowledgements

The presented work was made possible by the Marie Curie Initial Training Network wavetrain2, financed by the FP7 of the European Commission (contract-N° MCITN-215414).

The authors express their thanks to the Azores University (Eduardo Manuel Vieira de Brito de Azevedo / Centre of Climate, Meteorology and Global Changes) who kindly made available the data from the Azores wave buoys in the context of the CLIMAAT and CLIMARCOST Projects.

References

- [1] Centre of Climate, Meteorology and Global Changes of the Azores University. CLIMAAT and CLIMARCOST Projects.(FEDER-PIC-Interreg-IIIb,MAC2./A3-03/MAC/2.3/A5-05/MAC/2.3/A1).
- [2] Sarmento, A.J.N.A., Brito-Melo, A., 1996. An experiment-based time domain model of OWC power plants. International Journal of Offshore and Polar Engineering 6 (3), 227–233.
- [3] Delhommeau, G (1987). “Les problèmes de diffraction-radiation et de résistance de vagues: étude théorique et résolution numérique par la méthode des singularités,“ Thèse de Docteur ès Sciences, ENSM, Nantes.
- [4] Brito-Melo, A., Sarmento, A.J.N.A., Clément, A.H., Delhommeau, G., 1999. A 3D boundary element code for the analysis of OWC wave power plants. In: Proceedings of the Ninth International Offshore and Polar Engineering Conference, Brest, ISOPE, I., pp. 188–195.
- [5] Brito-Melo, A.; Hofmann, T.; Sarmento, A.J.N.A.; Clément, A.H. and Delhommeau, G., “Numerical Modeling of OWC-Shoreline devices including the effect of surrounding coastline and non-flat bottom”, Int. J. Offshore and Polar Engng., Vol. 11, No. 2, pp. 147-154.
- [6] Sarmento, A. J. N. A., Falcão A. F. de O., 1985. Wave generation by an oscillating surface-pressure and its application in wave-energy extraction, Journal of Fluid Mechanics, 150, 467-485.